ISSN 2347-3487

# Stagnation-Point Flow Towards a Heated Porous stretching Sheet Through a Porous Medium with Thermal Radiation and Variable Viscosity

Faiza A. Salama [a,b]

[a] Department of Mathematics, Faculty of Science and Arts, Qassim University, Al-Muznib, Saudi Arabia.

[b] Department of Mathematics , Faculty of Science , Suez Canal University, Egypt.

## Abstract.

An analysis is made for the steady two-dimensional stagnation-point flow in a porous medium of an incompressible viscous fluid towards a permeable stretching surface with variable viscosity and thermal radiation. The viscosity of the fluid is assumed to be an inverse linear function of the fluid temperature. The stretching velocity and the surface temperature are assumed to vary linearly with the distance from the stagnation point. The governing equations for the problem where changed to dimensionless ordinary differential equations using scaling group of transformations. The transformed governing equations in the present study were solved numerically by using Rung-Kutta and Shooting method. Favorable comparison with previously published work is performed. A comparison between the analytical and numerical solutions has been included. The numerical solutions are presented to illustrate the influence of the various values of the ratio of free stream velocity and stretching velocity, the viscosity variation parameter and the porosity parameter. These effects of the different parameter on the velocity and temperature profiles in the boundary layer as well as the coefficient of heat flux and shearing stress at the surface are presented graphically to show interesting aspects of the solution.

PACS: 47.15.Cb, 47.55.Mh, 44.40.+a

Council for Innovative Research

Peer Review Research Publishing System

Journal: JOURNAL OF ADVANCES IN PHYSICS

Vol. 11, No. 3

www.cirjap.com, japeditor@gmail.com

ISSN 2347-3487

## 1 Introduction.

The study of hydrodynamic flow and heat transfer over a stretching sheet becomes much more interesting due to its important applications in engineering and industry such as the extrusion of polymers, the cooling of metallic plates, the aerodynamic extrusion of plastic sheets, etc. Flow near a stagnation point in a plane was initiated by Hiemenz [1]. Ramachandran et al. [2] studied laminar mixed convection in two dimensional stagnation flows around heated surface. The stagnation point flows towards a surface which is moved or stretched have been considered for example by Chiam [3], Mahapatra and Gupta [4,5], Nazar et al. [6,7], Boutros et al. [8], Mahapatra et al. [9] and recently by Ishak et al. [10,11]. Gupta et al. [12] analyzed stagnation point flow towards a stretching surface. They reported in their research work that a boundary layer is formed when stretching velocity is less than the free stream velocity.

In many engineering areas processes occur at high temperatures so knowledge of radiation heat transfer beside the convective heat transfer play very important role and cannot be neglected. Rosseland approximation is used to describe the radiative heat flux in energy equation. Free convection heat transfer with radiation effect near the isothermal stretching sheet and over a flat sheet near the stagnation point have been investigated respectively by Ghaly et al. [13] and Pop et al [14]. Seddeek et al. [15] investigated theoretically effects of radiation and thermal diffusivity on heat transfer over a stretching surface with variable heat flux. Recently, Seddeek et al. [16] have considered analytical solution for the effect of radiation on flow of a magneto-micropolar fluid past a continuously moving plate with suction and blowing.

All the above studies were confined to the fluid with uniform viscosity. However, it is known that the fluid viscosity changes with temperature [17] for example the viscosity of water decreases by about 240% when the temperature increases from $10^0 C$ $(\mu = 0.013\,\mathrm{g\ cm^{-1}s^{-1}})$ to $50^0 C$ $(\mu = 0.00548\,\mathrm{g\,cm^{-1}s^{-1}})$. Therefore, to predict the flow behavior accurately it is necessary to take into account the viscosity variation for incompressible fluids. Anwar et al [18] and Barakat [19] and Rahman et al. [20] showed that, when the effect of variable viscosity is included the flow characteristics may changed substantially compared to the constant viscosity assumption . Also they found that the influence of variable viscosity vanishes for the limiting case of vanishing temperature differences $\Delta T = T_w - T_\infty$. In this study, we will investigate the structure of the boundary layer stagnation-point flow and heat transfer over a porous stretching sheet in porous medium in the presence of thermal radiation and variable viscosity. The viscosity of the fluid is assumed to vary as inverse linear function of temperature. The wall surface temperature is linearly proportional to the distance away from the origin. The governing partial differential equations have reduced to a system of ordinary differential equations by using Lie-group method [21]. The resulting system of non-linear differential equations is then solved numerically using shooting method coupled with Runge-Kutta scheme.

## 2. Mathematical analysis

Consider the steady boundary-layer flow near the stagnation point in a porous medium of viscous incompressible fluid at a surface coinciding with the plane y=0, the flow being in a region $y > 0$ where the space above the plane sheet is filled with the porous medium. The equal and opposite forces are applied along the x-axis so that the wall is stretched keeping the origin fixed. The velocity $u_w(x)$ and the temperature $T_w(x)$ of the stretching sheet is proportional to the distance x from the stagnation-point. We assume that the fluid properties are isotropic and constant, except for the fluid viscosity, $\mu$ , which is assumed to vary as an inverse linear function of temperature, T, in the form [22]

$$\frac{1}{\mu} = \frac{1}{\mu_\infty}[1+\gamma(T-T_\infty)] \text{ i.e. } \frac{1}{\mu} = \zeta(T-T_r), \tag{1}$$

Where, $\zeta = \gamma/\mu_\infty$ and $T_r = T_\infty - 1/\gamma$, with $\mu_\infty$ and $T_\infty$ being the fluid free stream dynamic viscosity and the fluid free stream temperature, and $\zeta$ and $T_r$ being constants, their values deepening on the reference state and thermal property of the fluid $\gamma$ . In general, $\zeta \succ 0$ for fluids such as liquids and $\zeta \prec 0$ for gases.

The governing equations of continuity, momentum and energy under the influence of variable viscosity with radiation in the boundary layer are

$$\frac{\partial \bar{u}}{\partial \bar{x}} + \frac{\partial \bar{v}}{\partial \bar{y}} = 0, \tag{2}$$

$$\bar{u}\frac{\partial \bar{u}}{\partial \bar{x}} + \bar{v}\frac{\partial \bar{u}}{\partial \bar{y}} = \bar{U}\frac{\partial \bar{U}}{\partial \bar{x}} + \frac{1}{\rho_\infty}\frac{\partial}{\partial \bar{y}}(\mu\frac{\partial \bar{u}}{\partial \bar{y}}) - \frac{\mu}{\rho_\infty K}(U - u_\infty), \tag{3}$$

$$\bar{u}\frac{\partial T}{\partial \bar{x}} + \bar{v}\frac{\partial T}{\partial \bar{y}} = \frac{k}{\rho_\infty c_p}\frac{\partial^2 T}{\partial \bar{y}^2} - \frac{1}{\rho_\infty c_p}\frac{\partial q_r}{\partial \bar{y}}, \tag{4}$$

ISSN 2347-3487

where $\bar{u}$ and $\bar{v}$ are the velocity components along x- and y-direction, T is the fluid temperature, $\rho_\infty$ is the fluid density, k is the thermal conductivity and K is the permeability of the porous medium. The quantity $q_r$ on the right hand side of the energy equation (4), represents the radiative heat flux in the y-direction. By using the Rosseland approximation (Raptis [23]) the radiative heat flux $q_r$ given by:

$$q_r = \frac{-4\sigma}{3k^*}\frac{\partial T^4}{\partial \bar{y}} \tag{5}$$

Where $\sigma$ is the Stefan-Boltzmann constant and $k^*$ is the Rosseland mean absorption coefficient. Assuming that the temperature differences within the flow is such that $T^4$ may be expanded in a Taylor series and expanding $T^4$ about $T_\infty$ and neglecting higher orders we get $T^4 \equiv 4T_\infty^3 T - 3T_\infty^4$. Therefore, the equation (4) becomes

$$\bar{u}\frac{\partial T}{\partial \bar{x}} + \bar{v}\frac{\partial T}{\partial \bar{y}} = \frac{k}{\rho_\infty c_p}\frac{\partial^2 T}{\partial \bar{y}^2} + \frac{16\sigma T_\infty^3}{3\rho_\infty c_p k^*}\frac{\partial^2 T}{\partial \bar{y}^2} \tag{6}$$

The boundary conditions are

$$\bar{u}(x) = c\bar{x},\ \bar{v} = -\bar{v}_w,\ T = T_w(\bar{x}) = T_\infty + b\bar{x} \quad \text{at} \quad \bar{y} = 0,$$
$$\bar{u} \to \bar{U}(\bar{x}) = a\bar{x},\ T \to T_\infty \quad \text{as} \quad \bar{y} \to \infty \tag{7}$$

where a,b,c are constants, and $\bar{v}_w$ is the wall velocity.

By introducing the following non-dimensional variables

$$x = \frac{\bar{x}}{\sqrt{\nu_\infty/c}},\ y = \frac{\bar{y}}{\sqrt{\nu_\infty/c}},\ u = \frac{\bar{u}}{\sqrt{\nu_\infty c}},\ v = \frac{\bar{v}}{\sqrt{\nu_\infty c}},\ U = \frac{\bar{U}}{\sqrt{\nu_\infty c}},\ \theta = \frac{T - T_\infty}{T_w - T_\infty} \tag{8}$$

Using (8), equations (2), (3) and (6) take the following dimensional form

$$\frac{\partial u}{\partial x} + \frac{\partial v}{\partial y} = 0, \tag{9}$$

$$u\frac{\partial u}{\partial x} + v\frac{\partial u}{\partial y} = U\frac{\partial U}{\partial U} - \frac{\theta_r}{\theta - \theta_r}\frac{\partial^2 u}{\partial y^2} + \frac{\theta_r}{(\theta - \theta_r)^2}\frac{\partial u}{\partial y}\frac{\partial \theta}{\partial y} - k_1\frac{\theta_r}{\theta - \theta_r}(U - u), \tag{10}$$

$$u\left(\frac{\partial \theta}{\partial x} + \frac{\theta}{x}\right) + v\frac{\partial \theta}{\partial y} = \frac{1}{Pr_\infty}\left(1 + \frac{4}{3R}\right)\frac{\partial^2 \theta}{\partial y^2}, \tag{11}$$

and the boundary conditions (7) take the form

$$u = x,\ v = -s,\ \theta = 1 \quad \text{at } y = 0,$$
$$u \to (a/c)\,x,\ \theta = 0 \quad \text{as } y \to \infty. \tag{12}$$

Where $pr_\infty = \upsilon_\infty \rho_\infty c_p / k$ is the ambient Prandtl number, $k_1 = \upsilon_\infty / Kc$ is the permeability parameter of the porous medium, $\theta_r = -1/\gamma(T_w - T_\infty)$ is the variable viscosity parameter, $R = kk^*/4\sigma T_\infty^3$ is the thermal radiation parameter and $s = -\bar{v}_w/\sqrt{c\nu_\infty}$ is the mass flux parameter (s>0 corresponds to suction and s<0 corresponds to blowing).

Equations (9), (10) and (11) are conveniently solved by introducing the stream function $\psi(x, y)$ defined by

$$u = \frac{\partial \psi}{\partial y},\ v = -\frac{\partial \psi}{\partial x} \tag{13}$$

ISSN 2347-3487

Which satisfy the continuity equation (9) automatically. Substituting $\psi(x, y)$ into the equation (10) and (11), we obtain

$$\frac{\partial\psi}{\partial y}\frac{\partial^2\psi}{\partial x\partial y}-\frac{\partial\psi}{\partial x}\frac{\partial^2\psi}{\partial y^2}=U\frac{\partial U}{\partial U}-\frac{\theta_r}{\theta-\theta_r}\frac{\partial^3\psi}{\partial y^3}+\frac{\theta_r}{(\theta-\theta_r)^2}\frac{\partial^2\psi}{\partial y^2}\frac{\partial\theta}{\partial y}-k_1\frac{\theta_r}{\theta-\theta_r}(U-\frac{\partial\psi}{\partial y}), \quad (14)$$

$$\frac{\partial\psi}{\partial y}(\frac{\partial\theta}{\partial x}+\frac{\theta}{x})-\frac{\partial\psi}{\partial x}\frac{\partial\theta}{\partial y}=\frac{1}{Pr_\infty}(1+\frac{4}{3R})\frac{\partial^2\theta}{\partial y^2}, \quad (15)$$

The boundary condition become

$$\frac{\partial\psi}{\partial y}=x\ ,\frac{\partial\psi}{\partial x}=s,\ \theta=1\quad \text{at } y=0,$$

$$\frac{\partial\psi}{\partial y}\to U=\frac{a}{c}x,\theta=0\quad \text{as } y\to\infty \quad (16)$$

We now introduce the simplified form of Lie-group transformations namely, the scaling group of transformations [24]:

$$\Gamma: x^*=xe^{\varepsilon\alpha_1},\ y^*=ye^{\varepsilon\alpha_2},\ \psi^*=\psi e^{\varepsilon\alpha_3},\ u^*=ue^{\varepsilon\alpha_4},\ v^*=ve^{\varepsilon\alpha_5},$$
$$U^*=Ue^{\varepsilon\alpha_6},\theta^*=\theta e^{\varepsilon\alpha_7} \quad (17)$$

Where $\alpha_1,\alpha_2,\alpha_3,\alpha_4,\alpha_5,\alpha_6$ and $\alpha_7$ are the transformation parameters and $\varepsilon$ is a small parameter.

Substituting equation(17) into equations (14) and (15), we obtain the invariance conditions

$$\alpha_1=\alpha_3-\alpha_4=\alpha_6,\alpha_2=\alpha_5=\alpha_7=0$$

These relations lead to the following differential equations(characteristic equations) for similarity:

$$\frac{dx}{\alpha_1 x}=\frac{dy}{0}=\frac{d\psi}{\alpha_1\psi}=\frac{du}{\alpha_1 u}=\frac{dv}{0}=\frac{dU}{\alpha_1 U}=\frac{d\theta}{0}$$

From these equations, we find the similarity transformations

$$\eta=y,\ \ \psi^*=xF(\eta),\ \ \theta^*=\theta(\eta). \quad (18)$$

Substituting these values in equations (14) and (15), we finally obtain the system of nonlinear ordinary differential equations

$$f'^2-ff''=(\frac{a}{c})^2-\frac{\theta_r}{\theta-\theta_r}f'''+\frac{\theta_r}{(\theta-\theta_r)^2}f'\theta'-k_1\frac{\theta_r}{\theta-\theta_r}(\frac{a}{c}-f') \quad (19)$$

$$(1+\frac{4}{3R})\theta''+Pr(1-\frac{\theta}{\theta_r})(f\,\theta'-f'\theta)=0 \quad (20)$$

Where $Pr=Pr_\infty(1-\frac{\theta}{\theta_r})^{-1}$ is the variable Prandtl number. The corresponding boundary conditions are

$$f'(0)=1,\ f(0)=s,\ \theta(0)=1,$$

$$f'(\infty)\to\frac{a}{c},\ \ \theta(\infty)\to 0. \quad (21)$$

In the above equations, a prime denotes differentiation with respect to $\eta$. In the case of $\frac{a}{c}=0$ and $\theta_r \to \infty$ (uniform viscosity), Eq. (19), together with the boundary conditions $f(0)=s,\ f'(0)=1,$ and $f'(\infty)=0$ has an exact solution in the form

$$f(\eta)=s+\frac{2}{s+\sqrt{s^2+4(1+k_1)}}[1-\exp(-\frac{\eta}{2}(s+\sqrt{s^2+4(1+k_1)}))].$$

The quantities of practical interest in this study are the skin friction coefficient $C_f$ and local Nusselt number $Nu_x$, which are defined as

$$C_f=\frac{2\mu}{\rho_\infty \bar{u}_w^2}(\frac{\partial \bar{u}}{\partial \bar{y}})_{\bar{y}=0};\quad Nu_x=\frac{q_w \bar{x}}{k(T_w-T_\infty)},\ q_w=k(1+\frac{4}{3R})(\frac{\partial T}{\partial \bar{y}})_{\bar{y}=0} \qquad (23)$$

Using equations (8), (18) and (23), the skin friction coefficient and the local Nusselt number can be expressed as

$$Re_x^{\frac{1}{2}}C_f=\frac{\theta_r}{\theta_r-1}f''(0),\qquad Re_x^{-\frac{1}{2}}Nu_x=-(1+\frac{4}{3R})\theta'(0) \qquad (24)$$

where $Re_x=\frac{\bar{u}_w(\bar{x})\bar{x}}{\nu_\infty}$ is the local Renolds number based on stretching velocity $\bar{u}_w(\bar{x})$.

From equation (1), $\mu$ can be readily put in the form

$$\mu=\mu_\infty/(1-(\theta(\eta)/\theta_r)) \qquad (25)$$

which clearly shows that, as $\theta_r \to \infty$ (or as $\gamma$=0) this leads to $\mu \to \mu_\infty$ (constant), i.e., the viscosity variation in the boundary layer is negligible. Also, according to the definition of viscosity/temperature parameter, $\theta_r=(T_r-T_\infty)/(T_w-T_\infty)$, for a given reference temperature $T_r$,variation of $\theta_r$ means in fact, variation of the temperature difference $\Delta T=T_w-T_\infty$. For the case of fluid heating $T_w \succ T_\infty$, Afify [25] showed that $\theta_r$ cannot take the values between zero and one and suggested that $\theta_r \succ 1$ for gases and $\theta_r \prec 0$ for liquids.

## 3. Results and Discussion.

The system of transformed differential equations, Eqs. (19) and (20), with the corresponding boundary conditions, Eq. (21) have been solved numerically by means of the fourth-order Runge-Kutta method with systematic estimates of $f''(0)$ and $\theta'(0)$ being made by using the shooting technique[26]. In the present calculations, step sizes of $\Delta\eta=0.01$ and $\eta_{max}=6$ were found to be satisfactory in obtaining sufficient accuracy within a tolerance of less than $10^{-7}$ in nearly all cases. In order to assess the accuracy of the present numerical method, we compared our numerical results obtained for the dimensionless stream function and its derivative taking $\frac{a}{c}=0$, and $\theta_r \to \infty$ in Eq. (19) with those obtained analytically. The numerical and the analytical values of $f(\eta)$ and $f'(\eta)$ for $k_1=0.5$ and s=1 are shown in Fig. (1). The numerical values of $f(\eta)$ and $f'(\eta)$ are in good agreement with the obtained analytical values.

Many results are obtained through out this work. A representative set of results is presented graphically in Figs.2-16 in order to explore the various physical aspects of the problem. Fig. 2 shows the viscosity distributions across the boundary layer for various values of a/c for both the case of constant and variable viscosity. As velocity ratio parameter a/c increases, the viscosity distribution decreases inside the boundary layer. For very large values of $\theta_r(\to\infty)$, the velocity ratio parameter has a negligible effect on the viscosity distribution along the stretching surface. This is due to the fact that as $\theta_r \to \infty$ the factor $\theta_r/(\theta_r-\theta)$ in equation (25) approaches its limiting values of 1 as $\mu=\mu_\infty$ i.e. the viscosity becomes uniform within the boundary layer and equals the ambient fluid dynamic viscosity. Figs. 3, 4 and 5 show typical profiles for the fixed vertical velocity $f(\eta)$, the horizontal velocity $f'(\eta)$ and temperature $\theta(\eta)$

for different values of $a/c$, respectively. We observe that as the velocity ratio parameter increases the profiles of $f(\eta)$ and $f'(\eta)$ increase, while the profiles of $\theta(\eta)$ decrease. Also, it is observed that the velocity in the case of uniform viscosity ( $\theta_r \to \infty$ ) is higher than that of variable viscosity ($\theta_r = 1.1$) for all values of $a/c > 1$ at all points. However, the opposite trend is seen for values of $a/c < 1$, which is due to the fact that inverted boundary layer is formed for $a/c < 1$ i.e. when free stream velocity is lesser than stretching sheet parameter. It is important to note that for $a/c = 1$, there is no formation of boundary layer because the fluid velocity equals to the velocity of the stretching sheet. Similar trend has also been observed for the case of impermeable surface by Pop et al. [14] and Sharma et al. [27] in the absence of porous medium.

Figs 6-9, respectively, depict the effects of the viscosity-variation parameter $\theta_r$ on the fluid viscosity, velocity (vertical and horizontal) and temperature distributions, for some values of a/c (a/c=0.2, 1, 2) in the boundary layer. From these figures it is observed that for $a/c < 1$, the viscosity and temperature distributions increase as $\theta_r$ increases whereas the velocity profiles $f(\eta)$ and $f'(\eta)$ decrease as $\theta_r$ increases. However, the opposite trend is obtained for $a/c > 1$. Also, the effects of the variable viscosity parameter are found to be more pronounced for a fluid with small velocity ratio parameter. For $a/c = 1$, increasing the variable viscosity parameter has no effect on the viscosity, velocity and temperature distributions.

The effect of the porosity parameter $k_1$ for various values of $a/c$ on viscosity, velocity and temperature distributions are shown in Figs. 10-13. We notice that for $a/c < 1$, the viscosity and the temperature increase with increasing $k_1$, but the velocity decreases. On the other hand, this trend is reversed by increasing porosity parameter $k_1$ for $a/c > 1$, The reason for such behavior is that when $a/c < 1$, increasing the porosity parameter $k_1$ tends to increase the viscous forces and decelerate the flow, thus decreasing the velocity profiles. On the other hand when $a/c > 1$, increasing the porosity parameter tends to decrease the viscous forces and accelerate the flow, thus increasing the velocity profiles. From these figures it can be also noticed that the porosity parameter effect is observed to be more pronounced at lower values of $a/c$ and $k_1$. It is also observed that the porosity parameter has no effect on the viscosity, velocity, and temperature distributions for the case of $a/c = 1$.

Fig. 14 illustrates the effect of Radiation parameter R on the temperature distributions inside the boundary layer for two values of $a/c = 0.2$ and $a/c = 2$. It is observed that the increase of radiation parameter R leads to an increase of temperature distributions. Therefore, higher values of R implies higher surface heat flux and thereby making the fluid become warmer. For very large values of R $(\to \infty)$, the temperature distributions approach a linear shape. It is also observed that the influence of R on $\theta(\eta)$ is more pronounced for lower values of $a/c$. Figs. 15 and 16 respectively, illustrate the variation of the local skin friction $Re_x^{\frac{1}{2}} C_f$ and the local Nusselt number $Re_x^{-\frac{1}{2}} Nu_x$ for various values of the viscosity variation parameter $\theta_r$ and $a/c$. As shown, the local friction coefficient $Re_x^{\frac{1}{2}} C_f$ and the local Nusselt number $Re_x^{-\frac{1}{2}} Nu_x$ increase with increasing $\theta_r$ when $a/c < 1$, while reverse behavior is observed when $a/c > 1$. For $a/c = 1$, the values of $Re_x^{\frac{1}{2}} C_f$ equal to zero and the values of $Re_x^{-\frac{1}{2}} Nu_x$ remains constant for all values of $\theta_r$ inside the boundary layer. The zero shear stress at the wall corresponds to the parallel flow since the stretching velocity cx of the surface equals the velocity ax of the free stream. This behavior is consistent with the results of the velocity and temperature distributions exhibited in Figs.7,8 and 9. Also, the local rate of friction coefficient and the local rate of heat transfer are highly affected by the viscosity parameter for small values of $\theta_r$ in both $a/c = 0.2$ and $a/c = 2$. However, for large $\theta_r$ the local friction coefficient and the local heat transfer profile asymptotically approach those for the constant viscosity case. It is interesting to note that the sign of the wall shear stress was shown to depend on $a/c$ and $\theta_r$. Therefore, the effects of the variable viscosity and velocity ratio parameters are expected to alter the momentum boundary layer significantly.

## References


[1] K. Himenz, J. dingl. Polytech. J. 326 (1911) 321-328.

[2] N. Ramachandran, T. S. Chen, B. F. Armaly, ASME J. Heat Transfer 110 (1988) 373-377.

[3] T. C. Chiam, J. Phys Soc. Jpn. 63 (1994) 2443-2444.
[4] T. R. Mahapatra, A. S. Gupta, Acta Mech. 152 (2001) 191-196.
[5] T. R. Mahapatra, A. S. Gupta, Heat Mass transf. 38 (2002) 517-521.
[6] R. Nazar, N. Amin, D. Filip, I. Pop, Int. J. Nonlinear Mech 39 (2004) 1227-1235.
[7] R. Nazar, N. Amin, D. Filip, I. Pop, Int. J. Eng. Sci. 42 (2004) 1241-1253.
[8] Y. Z. Boutros, M. B. Abd-el Malek, N. A. Badran, H. S. Hassan, Meccanica 41 (2006) 681-691.
[9] T. R. Mahapatra, S. Dholey, A. S. Gupta, Meccanica 42(2007) 263-272.
[10] A. Ishak, R. Nazar, I. Pop, Magnetohydrodynamics 42(2006) 17-30.
[11] A. Ishak, R. Nazar, I. Pop, Meccanica 41(2006) 509-518.
[12] A. S. Gupta, T. R. Mahapatra, Canadian J. of Chem. Eng. 81(2003) 258-263.
[13] A. Y. Ghaly, E. M. E. Elbarbary,J. of App. Mech. 2(2002) 93-103.
[14] I. Pop, S. R. Pop, T. Grosan, Technische Mechanic 25 (2004) 100-106.
[15] M. A. Seddeek, M. S. Abd-Elmeguid, Physics Letters A 348(2006) 172-179.
[16] M. A. Seddeek, S. N. Odda, M. Y. akl, M. S. Abd-Elmeguid, Comput. Material Sci. 45(2009) 423-428.
[17] H. Herwig, G. Wickern, Wärme-und Stoffübertragung, 20 (1986)47-57.
[18] M. D. Anwar Hossain, M. d. Sajjad, Int. J Thermal Sci. 39 (2000) 173-183.
[19] E. I. I Barakat, Acta Mechanica 169 (2004) 195-202.
[20] M.. M. Rahman, K. M. Salahuddin, Comm. Nonlinear Sci. Numer Simulat, 15 (2009) 2073-2085.
[21] T. Tapanidis, G. Tsagas, H. P. Mazmdar, Nonlinear Funct. Anal. Appli. 8(2003) 345-350.
[22] F. C. Lai, F. A. Kulacki, Int. Heat Mass Transfer 33(1990) 1028-1031.
[23] A. Raptis, Int. Commun. Heat Mass transfer 25 (1998) 289-295.
[24] T. Tapanidis, G. Tsagas, H. P. Mazumdar, Nonlinear Funct. Anal. Appl. 8 (2003) 345-350.
[25] A. A. Afify, Transport in Porous Media, 66 (2007) 391-401.
[26] J. K. Adams, d. F. Rogers, Computer-ading Heat Transfer, McGraw-Hill, New York, 1973.
[27] P. R. Sharma, G. Sing, Tammasat Int. J. Sc. Tech., 13(2008) 11-16.

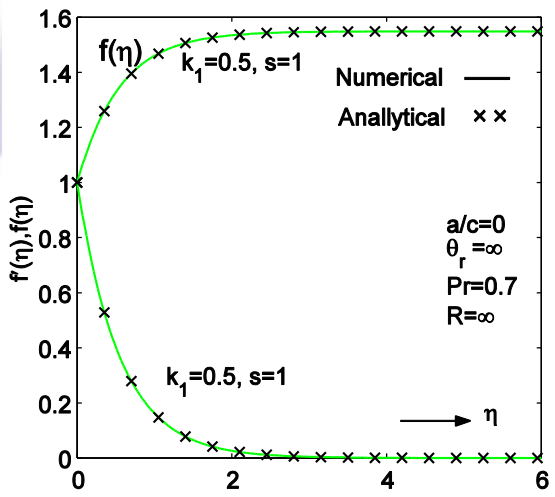


Fig. 1 Comparison of the exact solution and the numerical Solutions

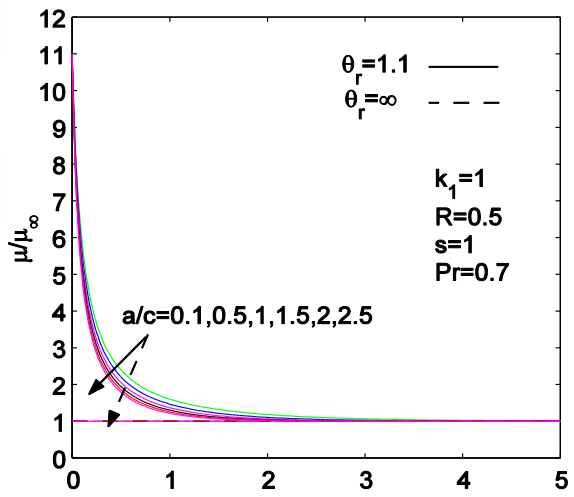


Fig. 2 Viscosity distribution for different values of a/c

ISSN 2347-3487

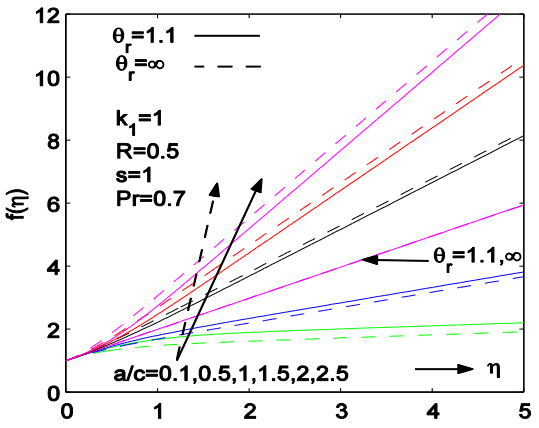


Fig. 3 Vertical velocity distribution for different values of a/c.

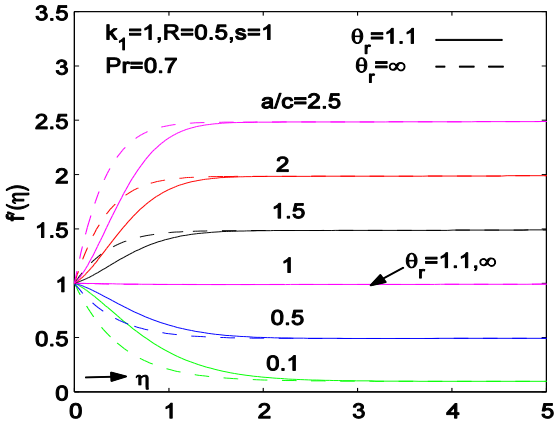


Fig. 4 Horizontal velocity distribution for different values of a/c.

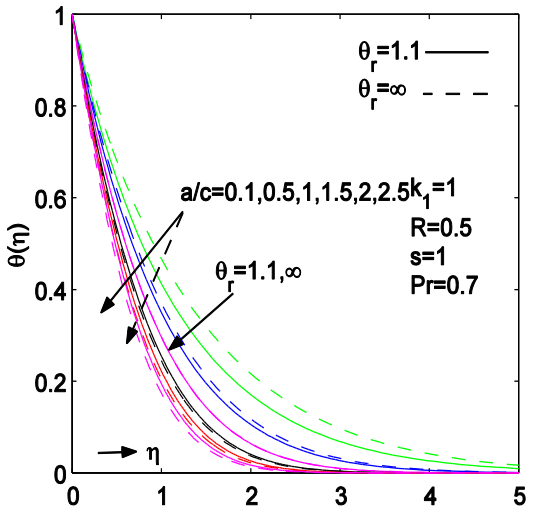


Fig. 5 Temperature distribution for different values of a/c.

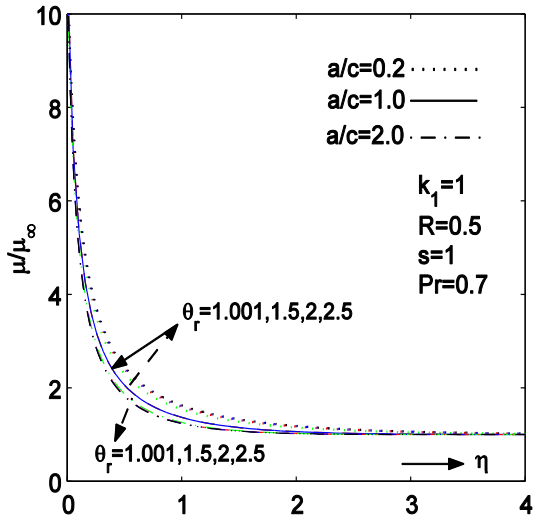


Fig. 6 Viscosity distribution for different values of $\theta_r$.

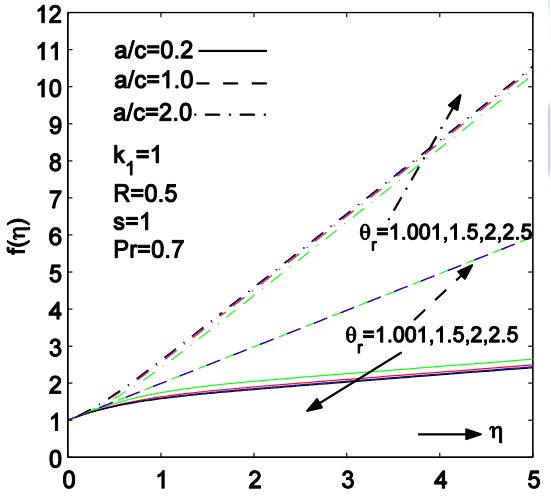


Fig. 7 Vertical velocity distribution for different values of $\theta_r$.

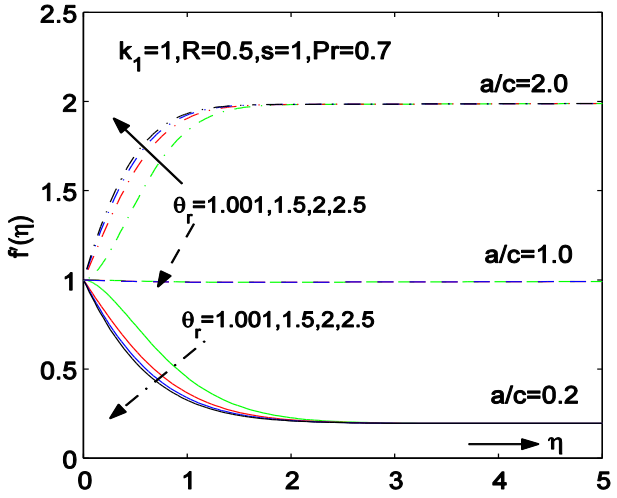


Fig. 8 Horizontal velocity distribution for different values of $\theta_r$.

ISSN 2347-3487

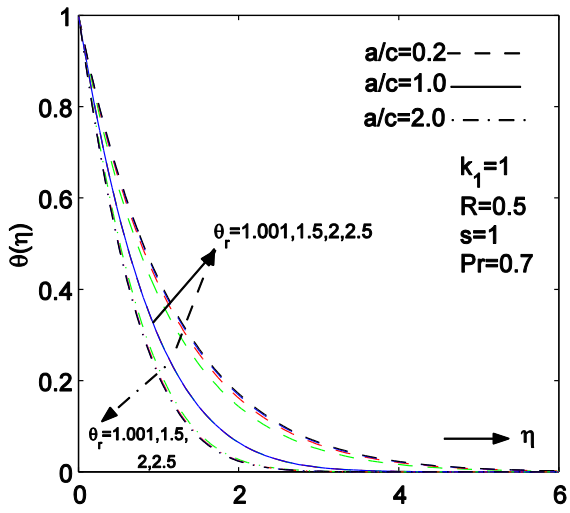


Fig. 9 Temperature distribution for different values of $\theta_r$

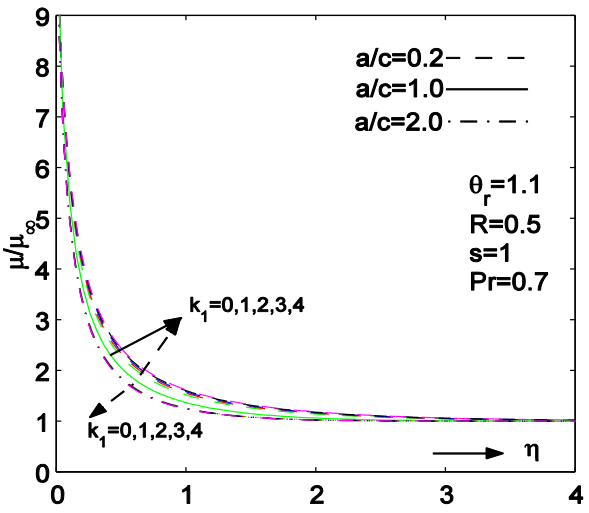


Fig. 10 Viscosity distribution for different values of $k_1$

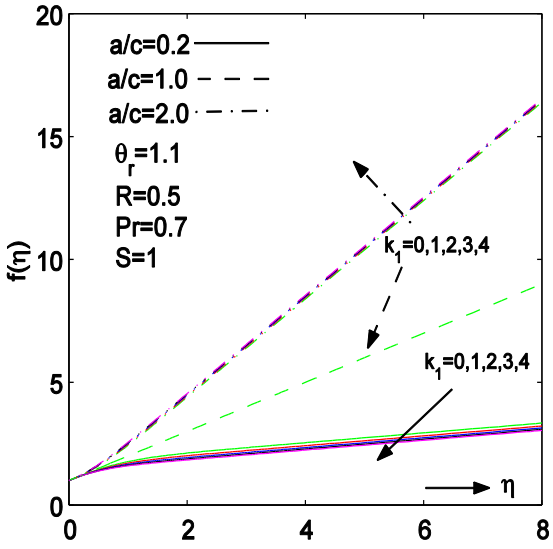


Fig. 11 Vertical velocity distribution for different values of $\theta_r$.

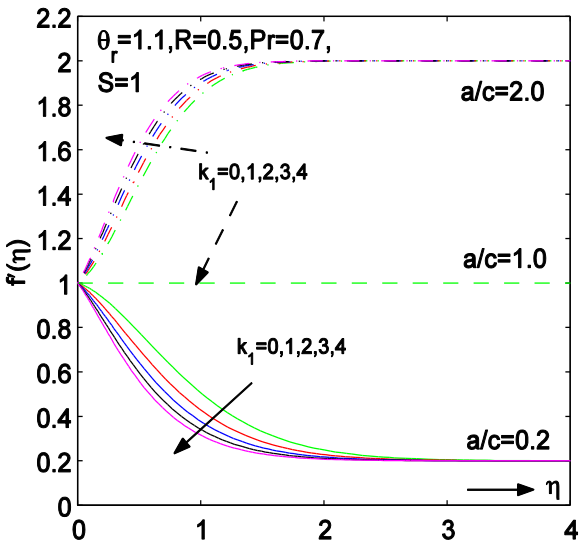


Fig. 12 Horizontal velocity distribution for different values of $\theta_r$.

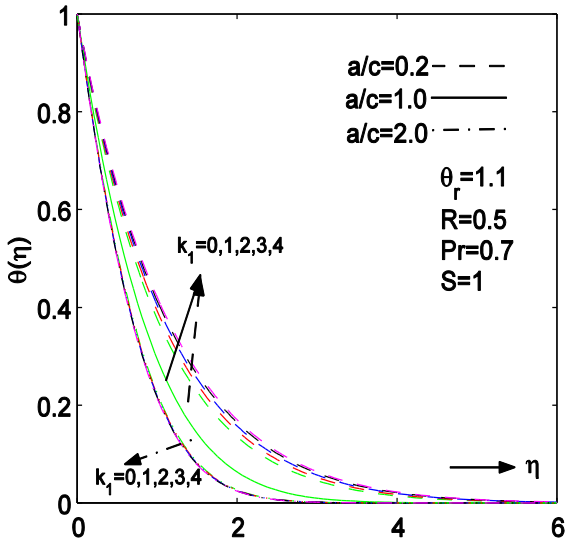


Fig. 13 Temperature distribution for different values of $k_1$.

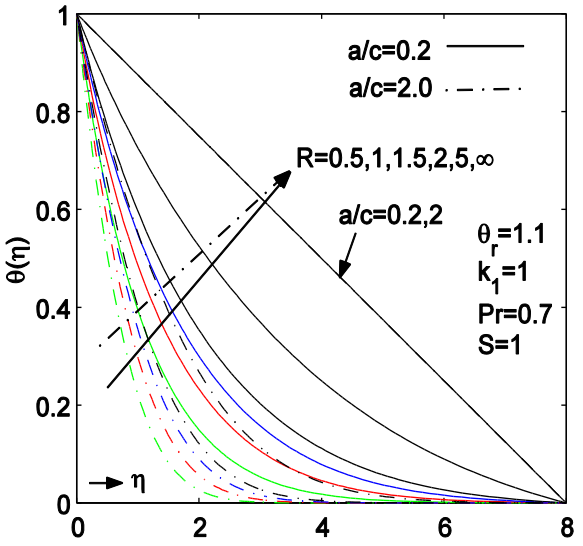


Fig. 14 Temperature distribution for different values of R.

ISSN 2347-3487

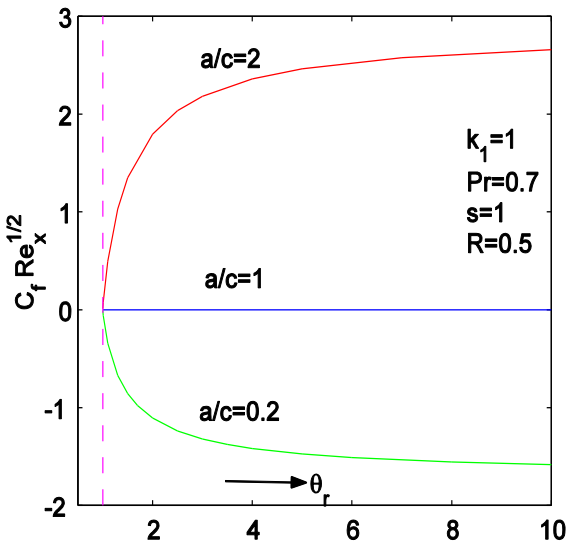


Fig.15 Variation of the skin friction coefficient $\theta_r$ for different a/c.

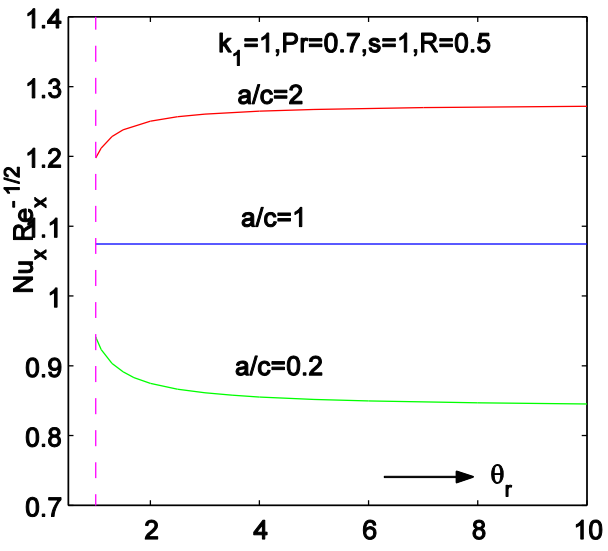


Fig.16 Variation of the local Nusselt Number with $\theta_r$ for different a/c.